



# Artificial Flexible Sensory Electronics Mimicking Human Somatosensory System

Seungjae Lee<sup>1</sup> · Hyejin Lee<sup>1</sup> · Geonyoung Jung<sup>1</sup> · Min Sub Kwak<sup>1</sup> · Young-Ryul Kim<sup>1</sup> · Hyunhyub Ko<sup>1</sup>

Received: 29 June 2024 / Revised: 29 August 2024 / Accepted: 30 August 2024

© The Author(s), under exclusive licence to Korean Institute of Chemical Engineers, Seoul, Korea 2024

## Abstract

Recent advancements in human–machine interfaces (HMIs), the Internet of Things (IoT), healthcare, and robotics have driven the need for technologies facilitating natural and intuitive interactions between users and devices. Central to this development are bio-inspired sensory electronics that emulate the sophisticated structures and functions of human sensory organs. This review comprehensively explores the latest advancements in flexible sensory electronics, which draw inspiration from the human somatosensory system, specifically tactile, auditory, and gustatory organs, to enhance user experiences in various applications. We discuss the underlying biological sensing mechanisms of each sensory organ and provide an overview of the materials, structures, and performances of devices that mimic them. For tactile sensors, we introduce fingertip-skin-inspired interlocked microstructures and mechanoreceptor-inspired multiple transduction modes that enable the detection and discrimination of static and dynamic tactile stimuli. In the auditory domain, we discuss cochlear-inspired acoustic sensors with frequency selectivity that allow for advanced sound processing and manipulation. Finally, artificial taste sensors integrated with taste receptor proteins or mimicking structures closely replicate human taste perception. The application of these human-inspired sensors in user-interactive interfaces, such as haptic-feedback rings for virtual reality, sound-driven robotics, and robotic taste-sensing systems, demonstrates their potential to revolutionize various fields. By understanding and mimicking biological sensory mechanisms, the development of artificial sensory electronics will continue to drive innovation in flexible sensory electronics and enhance user experiences through multimodal sensory integration.

**Keywords** Bio-inspired sensory electronics · Flexible sensor · Pressure sensor · Frequency-selective acoustic sensor · Taste sensor

## Introduction

There has been an emerging demand for the technologies allowing natural and intuitive interactions between users and devices for applications in human–machine interfaces (HMIs), the Internet of Things (IoT), healthcare, and robotics [1–3]. For instance, the involvement of all five human senses is crucial for reproducing all human experiences under a truly immersive environment in virtual reality (VR) and augmented reality (AR) applications. Such sensory integration with haptic feedback allows users to experience a more realistic and engaging virtual world, enhancing both

the user experience and practical applications of VR and AR technologies [4–6]. Recently, drawing inspiration from the structures and functions of sensory organs of living organisms, many bio-inspired sensors with great sensing performances have been reported [7–9]. Biological sensory organs, optimized through long evolutionary processes, exhibit outstanding sensitivity, selectivity, and adaptability. These characteristics make them ideal models for the development of bio-inspired sensory electronic devices. As depicted in Fig. 1, human sensory organs are categorized into five types: vision, hearing, olfactory, taste, and touch, each with unique structures and sensing mechanisms for perceiving and processing external stimuli. The development of bio-inspired electronics, which integrate touch, vision, hearing, olfactory, and taste sensors, addresses the growing need for natural and intuitive user–device interactions [10].

Among the five types of sensors, touch sensors play a crucial role by accurately perceiving input stimuli, which

✉ Hyunhyub Ko  
hyunhko@unist.ac.kr

<sup>1</sup> School of Energy and Chemical Engineering, Ulsan National Institute of Science and Technology (UNIST), Ulsan Metropolitan City 44919, Republic of Korea

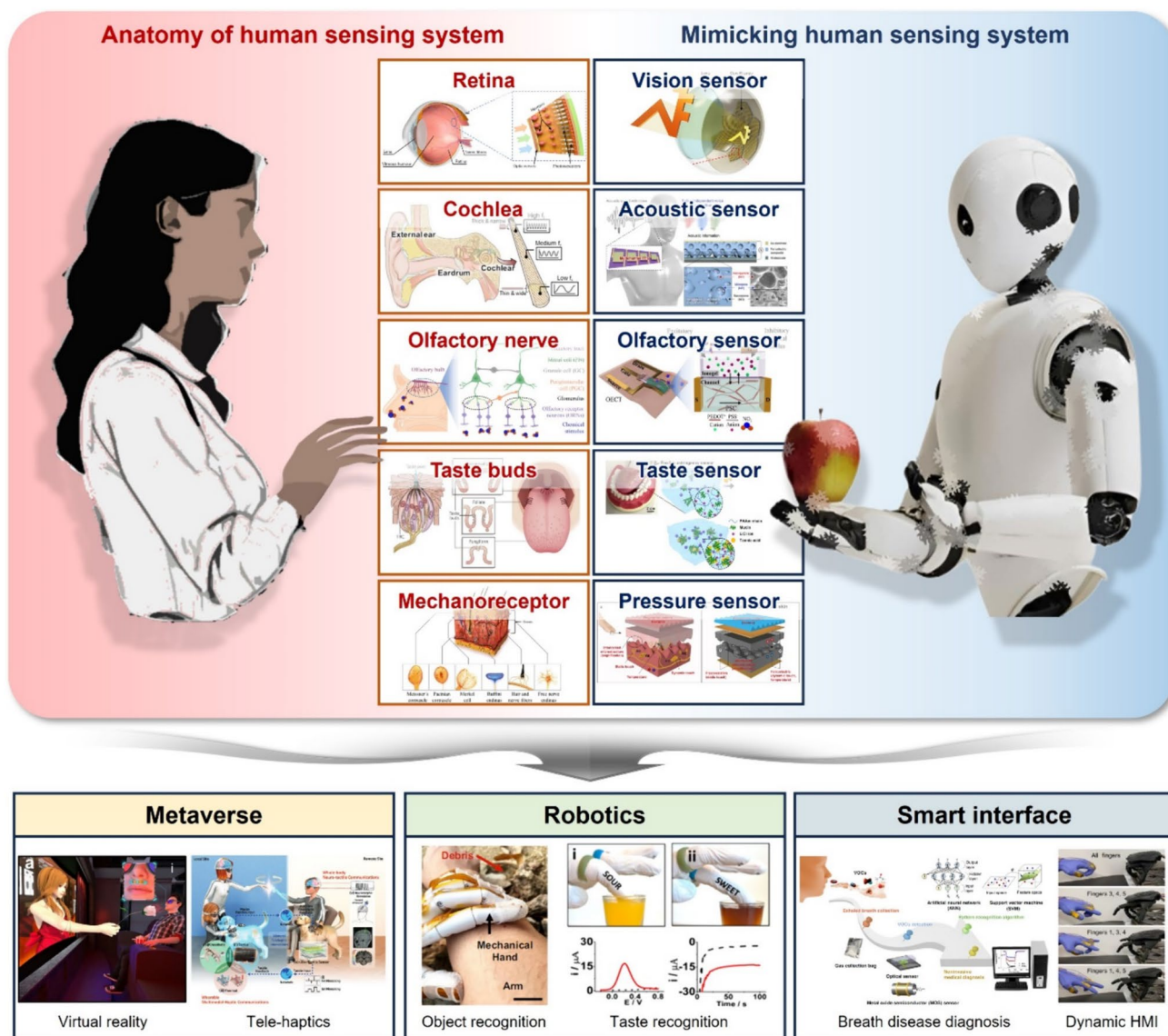


**Fig. 1** Overview of artificial sensory electronics mimicking human somatosensory system. (1) Anatomy of human sensing system: retina. Reproduced from Ref. [22]. Copyright 2020, Springer Nature. Cochlea. Reproduced from Ref. [45]. Copyright 2023, Wiley. Olfactory nerve. Reproduced from Ref. [25]. Copyright 2023, Springer Nature. Taste buds. Reproduced from Ref. [53]. Copyright 2006, Springer Nature. Mechanoreceptors. Reproduced from Ref. [31]. Copyright 2018, MDPI. (2) Mimicking human sensing system: vision sensor. Reproduced from Ref. [26]. Copyright 2017, Springer Nature. Acoustic sensor. Reproduced from Ref. [50]. Copyright 2022, American Association for the Advancement of Science. Olfactory sensor. Reproduced from Ref. [25]. Copyright 2023, Springer

Nature. Taste sensor. Reproduced from Ref. [65]. Copyright 2020, American Association for the Advancement of Science. Pressure sensor. Reproduced from Ref. [37]. Copyright 2015, American Association for the Advancement of Science. (3) Metaverse: virtual reality. Reproduced from Ref. [23]. Copyright 2023, Springer Nature. Tele-haptics. Reproduced from Ref. [4]. Copyright 2021, Wiley. (4) Robotics: object recognition. Reproduced from Ref. [24]. Copyright 2022, Springer Nature. Taste recognition. Reproduced from Ref. [14]. Copyright 2018, American Chemical Society. (5) Smart interface: breath disease diagnosis. Reproduced from Ref. [25]. Copyright 2023, Springer Nature. Dynamic HMI. Reproduced from Ref. [50]. Copyright 2022, American Association for the Advancement of Science

is a fundamental step enabling the provision of appropriate haptic feedback, ultimately allowing users to feel and manipulate virtual or remote objects with enhanced precision. [4, 11]. This is particularly important in applications such as VR gaming, teleoperation, and robotic surgery, where tactile sensing and feedback can greatly enhance

the user's sense of presence and control. Similarly, sound sensors enable voice control and command recognition in HMIs, enhancing robots' auditory perception for improved interaction [12, 13]. Taste sensors can enhance the capabilities of robots in food quality assessment and chemical analysis [14]. In healthcare, they contribute to disease

diagnosis and monitoring [15, 16]. Although the sense of taste has complexity of multisensory perception [17], artificial taste sensors are essential for detection and digitization of diverse taste information, enabling the potential implementation of gustatory sensations in virtual environments, thus enhancing immersive experiences in VR/AR [18, 19]. Artificial vision allows machines to perceive and interpret visual information, facilitating accurate tracking, object recognition, and seamless integration in VR/AR applications [20]. Vision sensors in human–machine interfaces enable gesture recognition, eye tracking, and facial expression analysis, fostering more natural interactions [21]. In addition, artificial visual sensor inspired by the hemispherical structure of retina has potential to achieve the high-performance artificial vision resolution, compared to that based on planar structure [22]. Olfactory sensors can detect specific scents, enabling scent-based emotional recognition in VR/AR [23], or enhancing the object recognition by detecting odor of various objects, combining with tactile sensing array without visual input [24]. In healthcare, olfactory sensors assist in disease diagnosis and monitoring by detecting, for example, specific volatile organic compounds [25]. The sophisticated structures and functions of these biological sensory organs provide significant inspiration for the development of next-generation sensors with high sensitivity, selectivity, and flexibility.

Among bio-inspired sensory electronics, vision-mimicking sensors have garnered significant attention due to the crucial role of vision in human perception, rapid technological advancements, and a wide range of applications [26, 27]. Conversely, research on olfactory-mimicking sensors has lagged behind other sensory-mimicking sensors, which can be attributed to the complexity of the human olfactory system, the vast diversity of odor molecules, and the subjective nature of odor perception [28, 29]. Technical challenges such as creating selective sensors, lack of standardization, limited reference materials, and the presence of interferents have also hindered the development of olfactory sensors. For those interested in a more comprehensive understanding of the current state-of-the-art technologies in artificial vision and olfactory systems, we recommend exploring dedicated reviews focusing on these specific sensory domains within the broader field of artificial sensory electronics [7, 9]. In contrast, recent advancements in sensor technologies and the growing demand for multisensory experiences have led to the increased interest in sensors mimicking touch, hearing, and taste. These sensory modalities offer unique opportunities for creating immersive and interactive user experiences by providing rich and intuitive feedback to users. As touch, hearing, and taste technologies continue to advance, they will drive future innovations in interactive interfaces, enabling richer

and more realistic user experiences through multimodal sensory integration.

This review focuses on the latest flexible sensory electronics that mimic the structures and functions of human tactile, auditory, and gustatory organs. We will introduce the biological sensing mechanisms of each sensory organ and provide a detailed overview of the structures, materials, and performances of the devices that emulate them. To consolidate key information, each section concludes with a table summarizing essential findings and characteristics of human mimicking sensors. Furthermore, we will discuss the potential applications and future development directions of these devices. In this way, we aim to provide insight into how biomimetic technology can drive innovation in flexible sensory electronics while also playing a significant role in various fields such as wearable devices, biosensors, and human–machine interfaces.

### Flexible Pressure Sensors Mimicking Human Mechanoreceptors

Humans perceive the tactile information by converting the external stimuli into electrical signals through biological mechanoreceptors. As depicted in Fig. 2a, when mechanical stimuli are applied to the epidermis layer, they activate four types of mechanoreceptors embedded in the dermis layer, each responding to different types of stimuli. Merkel cells and Ruffini's corpuscles respond to sustained pressure and low-frequency vibrations (0.5–30 Hz), as well as stretching and sustained pressure, and are classified as slow-adaptive (SA) types. In contrast, Meissner's corpuscles and Pacinian corpuscles effectively respond to low-frequency (10–50 Hz) dynamic skin deformation and high-frequency vibration (40–500 Hz) and are categorized as fast-adaptive (FA) types [30, 31]. These mechanoreceptors convert mechanical stimuli into electrical signals (action potentials) that are transmitted through the FA and SA afferent nerve fibers to the brain for further processing.

As the field of e-skin advanced, researchers began to recognize the importance of mimicking not only the sensory functions but also the intricate microstructures of human skin. Studies have shown that the presence of fingerprint-like patterns and interlocked microstructures between the epidermal and dermal layers play a crucial role in enhancing tactile sensitivity and efficiently transferring stimuli to mechanoreceptors [32]. Consequently, researchers have developed e-skins with bio-inspired microstructures, such as interlocked microdome [33], micropillar [34, 35], and pyramidal micropatterns [36], to improve pressure sensitivity and expand the dynamic range of sensing. However, many previous pressure sensors have been limited in their ability to fully mimic human mechanoreceptors. For instance, piezoelectric and triboelectric sensors excel at detecting dynamic

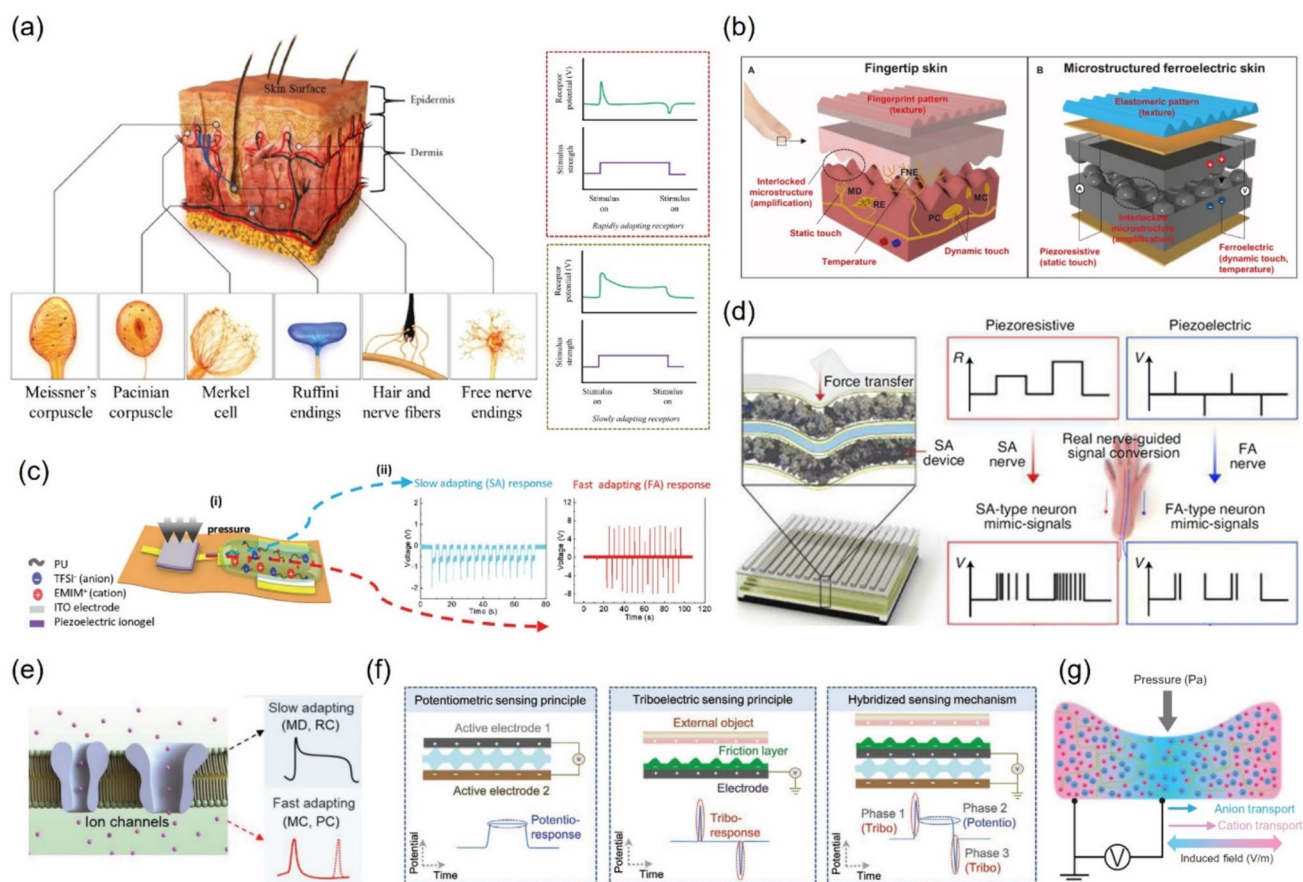


**Fig. 2** Flexible pressure sensors mimicking human mechanoreceptors. **a** Cross-sectional illustration of human skin featuring various mechanoreceptors corresponding with distinct SA/FA perception characteristics. Reproduced from Ref. [31]. Copyright 2018, MDPI. **b** Micro-structured ferroelectric skin emulating interlocked microridge structure of human skin with a fingertip pattern. Reproduced from Ref. [37]. Copyright 2015, American Association for the Advancement of Science. **c** Artificial SA/FA mechanoreceptors utilizing piezoelectric-ionic and piezoelectric transduction mechanisms. Reproduced from Ref. [38]. Copyright 2023, Wiley. **d** Action potential-driven synapse inspired tactile sensor, converting SA/FA

signals into spike patterns. Reproduced from Ref. [39]. Copyright 2021, Springer nature. **e** Ion-channel gating inspired mechanoreceptor sensor, integrating piezoelectric and ion channel system for FA/SA signals. Reproduced from Ref. [40]. Copyright 2018, Wiley. **f** Single-mode, self-powered mechanoreceptors combining triboelectric and potentiometric principles for FA/SA adaption. Reproduced from Ref. [43]. Copyright 2020, Wiley. **g** Piezoionic mechanoreceptors imitating the human somatosensory system. Reproduced from Ref. [44]. Copyright 2022, American Association for the Advancement of Science

stimuli with high frequency, but they cannot maintain signals under static conditions, rendering static pressure detection impossible. In contrast, piezoresistive and capacitive sensors effectively detect the static pressure but lag in responding to high-frequency inputs due to their slower response times. Therefore, these sensors can detect either static or dynamic pressure, depending on their transduction mechanisms, but not both simultaneously.

This limitation has hindered the development of sensors capable of detecting and differentiating between static and dynamic tactile stimuli with high sensitivity. To overcome these limitations, researchers have sought to develop sensors that can mimic human mechanoreceptors, enabling the sensing of both static and dynamic pressures in a single

device. Hybrid sensors with multiple signal transduction modes have emerged as a promising solution, as they can be independently sensing static and dynamic forces. Drawing inspiration from the concept of FA and SA mechanoreceptors, Park et al. developed a microstructured ferroelectric skin that can discriminate between static and dynamic tactile stimuli [37]. The key feature of this e-skin lies in its design, which includes microstructured ferroelectric films made from reduced graphene oxide (rGO)/poly(vinylidene fluoride) (PVDF) composites with interlocked microdome arrays and fingerprint-like microridges on their surface. This unique structure enhances the piezoelectric, pyroelectric, and piezoresistive sensing capabilities of the films for static and dynamic tactile and thermal signals. The interlocked

microdome arrays improve pressure sensitivity and temperature sensing, while the fingerprint-like microridges enhance texture perception. The rGO/PVDF composites enable piezoelectric and pyroelectric properties for detecting dynamic touch and temperature. By mimicking the structure and functions of human fingertip skin, this e-skin can simultaneously detect and discriminate between multiple tactile stimuli, including static and dynamic pressure, temperature, and vibration (Fig. 2b). In addition, the signal transduction of human sensation is based on the ion movement. Therefore, it is important to reduce the impedance from signal transduction difference between human skin and wearable devices. To achieve it, Huynh et al. demonstrated bio-inspired artificial FA and SA mechanoreceptors using piezoelectric and piezoelectric-ionic coupling effects [38]. The FA sensor is based on a piezoelectric poly(vinylidene fluoride-trifluoroethylene)(P(VDF-TrFE)) thin film, while the SA sensor is based on a P(VDF-TrFE) and 1-ethyl-3-methylimidazolium (EMIM-TFSI) ionogel. Furthermore, the researchers integrated these self-powered FA/SA sensors with synaptic electrolyte-gated field-effect transistors (EGFETs) to create artificial neuromorphic perception systems, paving the way for more advanced and human-like sensing capabilities in electronic skin devices (Fig. 2c).

In addition to the role of mechanoreceptors in independently detecting stimuli, there has been active research on developing tactile sensors that mimic the sensory transmission mechanisms based on action potential-driven synapses and ion channel gating. Figure 2d shows a system composed of particle-based polymer composite sensors that selectively respond to pressure and vibration, mimicking the SA and FA mechanoreceptors in human skin [39]. These sensors are fabricated by incorporating SA-mimicking rGO sheets and FA-mimicking BaTiO<sub>3</sub> nanoparticles into a polydimethylsiloxane (PDMS) matrix. The rGO sheets provide piezoresistive responses to static pressure, while the BaTiO<sub>3</sub> nanoparticles generate piezoelectric responses to dynamic pressure or vibration. Furthermore, an artificial finger is developed by integrating the sensors with a ridge-patterned structure mimicking the human fingerprint. The SA/FA data collected by each sensor is converted into spike patterns similar to action potentials. When combined with a deep learning algorithm, the artificial finger can learn, classify, and predict fine and complex textures. This novel tactile skin system represents a significant advancement in reproducing the human tactile sensing mechanism through the seamless integration of bio-inspired materials, structures, and signal processing. For achieving the ion channel gating mechanism, Fig. 2e demonstrates a self-powered cutaneous mechanoreceptor sensor by integrating a piezoelectric film (PVDF) for generating FA signals and an ion channel system (comprising a polyaniline solution and a porous membrane) to generate SA signals. In this system, ions flow through the pores in response to

external static pressure, mimicking the ion flux through a mechanosensitive ion channel membrane. This ability enables the simultaneous detection of static and dynamic pressure with high sensitivity [40].

Previous works on mechanoreceptors often faced limitations such as complicated device structures [40], multiple sensing elements requiring separate measurement setups, and increased power consumption [41, 42]. While some advancements have enabled the simultaneous detection and discrimination between static and dynamic stimuli, these solutions were not without their drawbacks, hindering their widespread application and practical use. To overcome these challenges, Wu et al. advanced the field by fabricating a single-mode, self-adapting, and self-powered mechanoreceptor that mimics both SA and FA responses within a single composite material, building on the concept of combining different signal transduction mechanisms [43]. This approach simplifies the fabrication process while maintaining the desired functionality. The device consists of a microstructured friction layer (PDMS) for the triboelectric component and a microstructured electrolyte (PVA/NaCl/Gly) for the potentiometric component. When subjected to mechanical stimuli, the potentiometric sensing mode generates a sustained response, while the triboelectric mode produces instantaneous voltage spikes at the beginning and end of the stimulation. The hybridization of these two sensing principles results in a single-mode voltage output that inherits both static and dynamic pressure-sensing characteristics, enabling the detection and discrimination of complex stimuli (Fig. 2f).

While the aforementioned studies focus on mimicking the human somatosensory system using artificial materials and structures, Dobashi et al. take a different approach by investigating the fundamental operating principles of biological mechanoreceptors (Fig. 2g). The human somatosensory system primarily operates through ionic currents across the ionic channel membrane to detect stimuli, transmit signals, and perceive tactile information. Inspired by this mechanism, Dobashi et al. present piezoionic mechanoreceptors based solely on ion movements, investigating hydrogel-based pressure sensors that generate ionic currents through the displacement of mobile protons when subjected to pressure. The authors create a gradient of fixed charges within the hydrogel by patterning films with varying concentrations of acrylic acid monomers, mimicking the resting potential across a cell membrane. This ion gradient enhances the piezoionic response and allows modulation of the dynamic range, enabling the sensors to discriminate between static and dynamic pressure stimuli. By adjusting the properties of hydrogels, the mechanoreceptors exhibit response times ranging from milliseconds to hundreds of seconds, mimicking the behavior of rapid- and slow-adapting mechanoreceptors in the human body [44] (Table 1)

**Table 1** Summary of human mechanoreceptor-inspired pressure sensor

Signal transduction (FA/SA)	Material	Device structure	Sensitivity	Pressure range	References
Piezoelectric/piezoresistive	Poly(vinylidene fluoride) (PVDF) (FA)/reduced graphene oxide (rGO) (SA)	Interlocked microdome structure with microridge pattern	–	0.6 Pa–49.5 kPa < 17.15 kPa 0.1–1000 Hz	[37]
Piezoelectric/piezoelectric-ionic coupling	Poly(vinylidene fluoride) (PVDF) (FA)/[EMM] [TFSI]* (SA)	Sandwich structure	35 $\mu$ A/Pa (< 2.45 kPa) 5 $\mu$ A/Pa (2.45–17.15 kPa) $V_{OC}$ : 0.7–1.2 V (static pressure)	< 14 kPa	[38]
Piezoelectric/piezoresistive	Polydimethylsiloxane (PDMS)/BaTiO <sub>3</sub> (FA)/reduced graphene oxide (rGO) (SA)	Sandwich structure with microridge pattern	– –	0.1–100 kPa (Pressure) 0.1–100 kPa (pressure) 1–1000 Hz (frequency)	[39]
Piezoelectric/ionic	Au/PVDF (FA)  Polyaniline (PANI) solution/pore membrane (SA)	Sandwich structure Fingerprint-like electrolyte	– 0.21 V/kPa (at 0.5 kPa) 0.38 V/kPa (at 0.5 kPa) – 0.349 V/kPa (at 0.5 kPa)	< 10 kPa	[40]
Triboelectric/potentiometric	PDMS (FA) Poly(vinyl alcohol)/sodium chloride/glycerol (SA)	Micro-structured triboelectric layer/electrolyte	~ 17 mV/N (potentiometric) ~ 20 mV/N (triboelectric)	0.01–10 N	46
Piezoionic	Polyacrylamide (pAAm) swollen with electrolytes/poly(acrylic acid-co-acrylamide) (poly(AA-co-AAm))	Piezoionic mechanoreceptor array (poly(AA-co-AAm) hemisphere)	8 $\mu$ V/kPa (< 360 kPa)	< 360 kPa	[44]

\*1-ethyl-3-methylimidazolium bis(trifluoromethylsulfonyl)imide

\*\*Poly(vinylidene fluoride-co-hexafluoropropylene)

## Frequency-Selective Acoustic Sensors Mimicking Human Cochlear

The human auditory sensory system consists of the external ear, eardrum, and cochlea, which work together to achieve mechanical amplification, vibration, and frequency selectivity (Fig. 3a). When sound waves travel through the air to the human ear, the external ear gathers and amplifies the sound pressure, causing the eardrum to vibrate. This vibration is then transferred to the lymph fluid and basilar membrane in the cochlea. The unique structure of the basilar membrane, with varying thickness, width, and modulus, allows for frequency selectivity as different frequencies cause vibrations in specific regions. The vibration of the basilar membrane tilts hair cells in the organ of Corti, which opens ion channels and transmits signals to the brain [45]. As like, the human ear's sound sensing mechanism has inspired the development of various artificial acoustic sensors that aim to replicate its structure and function. The human ear consists of three main parts: the outer ear, middle ear, and inner ear. Each part plays a crucial role in the process of converting sound waves into electrical signals that the brain can

interpret. One approach mimics the middle ear's structure and function, where researchers have developed a bionic eardrum using a thin, flexible piezoelectric membrane that vibrates in response to sound waves and generates electrical signals [46]. Another approach replicates the inner ear's cochlea, which is lined with thousands of tiny hair cells sensitive to different sound frequencies. Mimicking the hair cell structure, flexible acoustic sensors have been demonstrated, allowing the device to amplify the sound signals and detect a wide range of frequency range covering the human audible range [47, 48].

Artificial acoustic sensors have been utilized for various applications, including human-machine interfaces and hearing aids. In human-machine interfaces, these sensors enable voice-controlled systems and improve speech recognition accuracy. Hearing aids utilize artificial acoustic sensors to amplify and process sound, enhancing the hearing experience for individuals with hearing loss. Despite advancements in artificial acoustic sensors, several limitations exist. These sensors often struggle to perform well in noisy environments, leading to reduced sensitivity and selectivity. In addition, many artificial acoustic sensors lack the ability

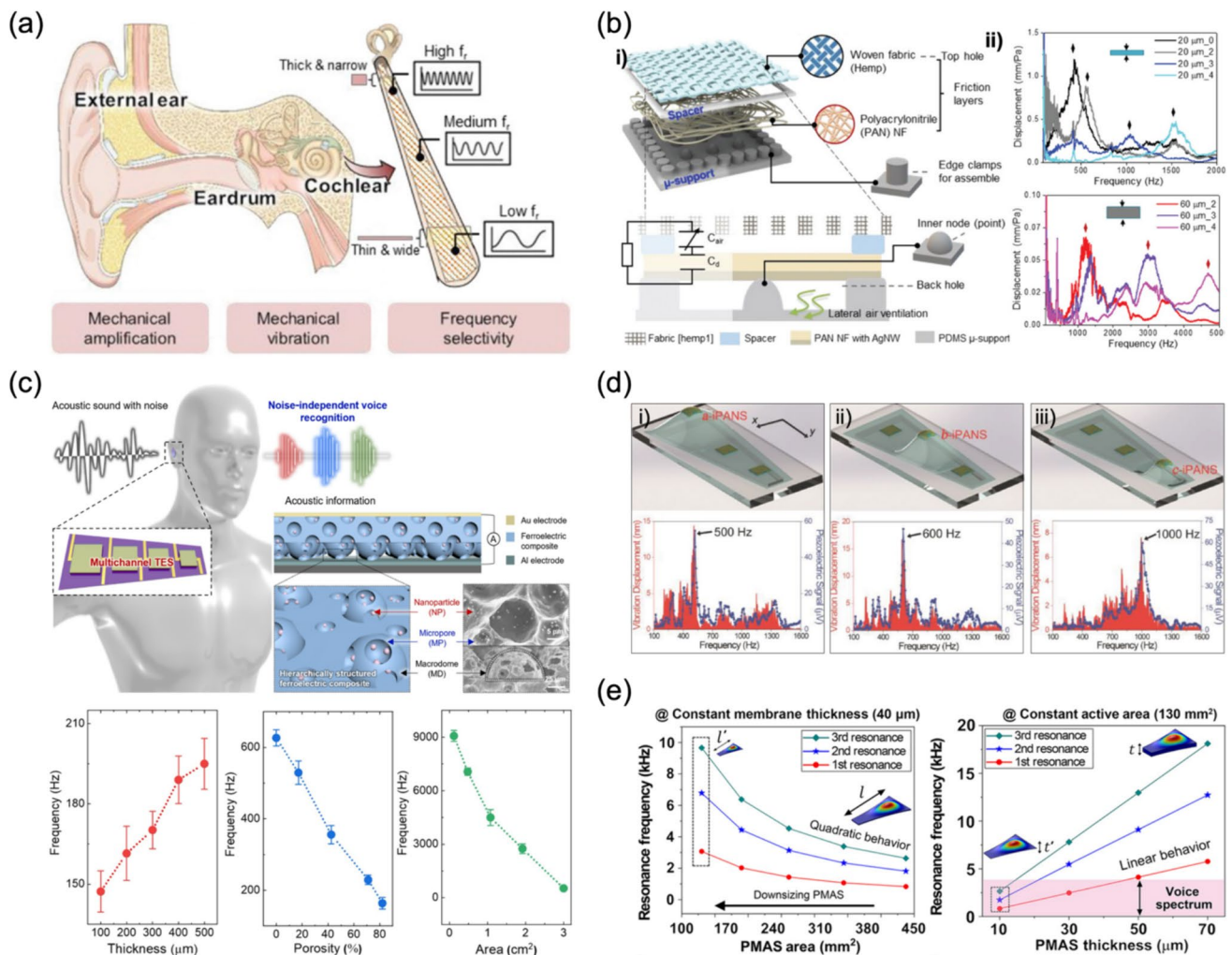


**Fig. 3** Frequency-selective acoustic sensors mimicking human cochlear. **a** Compositions of human ear and hearing process. **b** Self-powered, miniaturized artificial membrane (smBM) with broad frequency range. Reproduced from Ref. [45]. Copyright 2023, Wiley. **c** Frequency-selective triboelectric acoustic sensors with hierarchically structured composite. Reproduced from Ref. [50]. Copyright 2022,

American Association for the Advancement of Science. **d** Flexible inorganic piezoelectric acoustic sensors with frequency selectivity by their positions. Reproduced from Ref. [51]. Copyright 2014, Wiley. **e** Multiresonant frequency range determined by sensor area and thickness. Reproduced from Ref. [52]. Copyright by 2021, American Association for the Advancement of Science

to self-power and require external energy sources, limiting their practicality in real-world applications. This section will focus on the research for trying to overcome aforementioned issues with frequency-selective artificial cochleae inspired by the human cochlea. Frequency selectivity allows the ear to detect specific acoustic vibrations from a wide range of frequencies, enabling us to focus on and recognize a desired sound among the complex background noise [49]. These artificial cochleae aim to mimic the frequency selectivity of the human auditory system, facilitating the development of more advanced and efficient sensor technologies that can selectively detect and process specific frequencies. By understanding and applying the principles of the frequency selectivity of human cochlea, researchers can create innovative sensor systems with improved signal processing

capabilities, enhanced noise reduction, and better overall performance in a wide range of applications, from hearing assistance devices to user-interactive interfaces.

Conventional multi-resonant acoustic devices struggle to achieve broad and adjustable frequency selectivity within a compact footprint, hindering the realization of miniaturized and self-powered artificial BMs that mimic human hearing performance. To address these limitations, Lee et al. present a novel approach to developing a self-powered and miniaturized artificial basilar membrane (smBM) with broad frequency selectivity (Fig. 3b). By introducing inner boundary conditions (iBCs) through a micropatterned elastomeric support ( $\mu$ -support) and a porous nanofiber (NF) mat diaphragm, they achieve an adjustable multi-resonant spectrum in a compact device footprint. This innovative design enables

all-in-one fabrication and eliminates the need for integrating individual acoustic sensors of varying sizes, offering a significant advancement in the development of human-inspired acoustic sensing technologies for applications such as hearing aids and human–machine interfaces [45].

For dynamic HMIs, it requires the controllable resonance frequency for achieving the dynamic response responding to desired frequency recognition while canceling the undesired noise frequency. Despite the development of frequency-selective acoustic sensors, however, the narrow tunable range of resonance frequency selectivity with low sensitivity is still challenging. Park et al. developed a highly sensitive and linear triboelectric sensor (TES) with a wide range of frequency selectivity for dynamic human–machine interfaces (Fig. 3c). Mimicking the basilar membrane’s spatial variations in mechanical properties that enable selective detection of specific frequencies, the authors achieved frequency selectivity in their TES by tuning the resonance frequency through the structural design of hierarchical ferroelectric composites. By controlling the porosity, pore size, thickness, and overall sensor size, they demonstrated a wide tunable range of resonance frequencies from 145 to 9000 Hz, covering the human audible frequency range. This bio-inspired approach to frequency selectivity, mimicking the spatial frequency mapping of cochlea, enables the development of multichannel acoustic sensors that can selectively detect and amplify specific frequencies while minimizing the influence of noise. This ability allows for advanced human–machine interfaces with noise-independent acoustic sensing capabilities [50].

Building upon the concept of mimicking the human cochlea, Lee et al. developed a flexible inorganic piezoelectric acoustic nanosensor (iPANS) inspired by the human cochlear hair cells to address the limitations of existing artificial cochleae, such as insufficient electrical output and lack of flexibility (Fig. 3d). Their solution involved coupling a thin film of lead zirconate titanate (PZT), an

inorganic piezoelectric material with high piezoelectric constants, with a trapezoidal silicone-based membrane (SM) that mimics the function of the basilar membrane in the cochlea for frequency selectivity. The SM vibrates at different locations depending on the frequency of incoming sound waves, while the attached iPANS converts these vibrations into electrical signals. Although further miniaturization is necessary for practical application, this bio-inspired approach, leveraging the high piezoelectric performance of inorganic materials and the frequency selectivity of the SM, represents a significant step towards the development of efficient artificial cochleae for treating hearing loss [51].

Meanwhile, previous works faced challenges in covering the entire voice spectrum with limited channels and broadening the resonant spectrum to fully cover phonetic frequencies while downscaling resonant piezoelectric acoustic sensors. To overcome these limitations, Wang et al. demonstrated biomimetic frequency band control and sensitivity improvement of miniaturized piezoelectric mobile acoustic sensors (PMAS) (Fig. 3e). They developed a PMAS using an ultrathin piezoelectric membrane (~10 μm thick), mimicking the human BM. A 4.8-μm-thick polyethylene terephthalate (PET) membrane with a low-quality factor was employed to broaden the resonant bandwidth of the lead zirconate titanate (PZT) thin film, covering the entire voice spectrum. The thickness of the PZT membrane was optimized to minimize residual compressive stress and align lateral dipoles along the interdigitated electrode direction, enhancing sensitivity. The PMAS achieved a sensitivity of merit of 52 mV/Pa in a 130-mm<sup>2</sup> area, outperforming previous reports. Machine learning-based biometric authentication was demonstrated by integrating the PMAS with an algorithm processor and a customized Android app, achieving a 56% reduction in error rate compared to a conventional microelectromechanical system microphone [52] (Table 2)

**Table 2** Summary of frequency-selective acoustic sensors mimicking human cochlear

Signal transduction	Materials and structure	Sensitivity	Frequency detectable range	Frequency selectivity	References
Triboelectric	PAN* nanofiber as diaphragm supported by micropatterned PDMS	0.224 mV/Pa (at 1 kHz)	400–3000 Hz	330–3300 Hz (sensor) 423.4–3087.1 Hz (4-channel array)	[45]
Triboelectric	Hierarchical PVDF-TrFE**/BT composite	607 mV/Pa 33–56 dB	80–20,000 Hz	145–9000 Hz	[50]
Piezoelectric	Trapezoidal PZT/PET membrane	55 μV	100–1600 Hz	500, 600, and 1000 Hz	[51]
Piezoelectric	Trapezoidal PZT/PET membrane	40 mV/Pa·cm <sup>2</sup> – 28 dBV (at 830 Hz)	100–4000 Hz	830, 1840, and 2890 Hz	[52]

\*Polyacrylonitrile

\*\*Polyvinylidene fluoride-trifluoroethylene



## Taste Sensors Mimicking Human Gustatory System

The human gustatory system perceives five basic tastes through distinct mechanisms involving specific receptors and signaling pathways [53]. Sweet, bitter, and umami tastes are detected through G protein-coupled receptors (GPCRs). When activated by their respective taste molecules, these receptors initiate intracellular signaling cascades that lead to the release of neurotransmitters [54, 55]. In contrast, salty and sour tastes are detected through ion channel-mediated mechanisms, where taste substances directly interact with specific ion channels, causing changes in the membrane potential and triggering neurotransmitter release [53]. By mimicking the natural taste-sensing mechanisms, researchers can design artificial receptors and signaling pathways that selectively respond to specific taste compounds, enabling the creation of highly sensitive and selective taste sensors.

To achieve this goal, various approaches have been employed such as 2D materials, ion gels, and cell-based biosensors. 2D materials such as graphene and MoS<sub>2</sub> are atomically thin substances with high reactivity and excellent electrical properties, making them useful for constructing highly sensitive electronic tongues (E-tongues) [56]. Cell-based biosensors integrate real biological elements into E-tongues, achieving high selectivity [57]. Ion gels possess ionic conductivity and mechanical flexibility, making them suitable for the development of flexible and durable wearable taste sensors [58]. These materials are leveraged to detect taste substances by converting their interactions into electrical signals through sensing mechanisms such as triboelectricity [59, 60], potentiometry [61], impedance spectroscopy [62], and field-effect modulation [63]. These advancements allow for the development of advanced taste sensors with enhanced specificity, sensitivity, and neuromorphic computing capabilities.

Conventional taste sensors mimic the human gustatory system using a decoupled sensor array and a separate pattern recognition system, corresponding to gustatory receptor neurons and the gustatory cortex, respectively. However, these taste sensors have several limitations such as heavy hardware requirements and high-energy consumption, which hinder their practical implementation in IoT and mobile devices. To address these limitations, Han et al. developed an artificial gustatory neuron that mimics the human gustatory system (Fig. 4a). The researchers implemented the neuron using a metal–oxide–semiconductor field-effect transistor (MOS-FET) with an extended gate structure, which serves as a bioreceptor. They demonstrated pH-sensitive and sodium-sensitive neurons using Al<sub>2</sub>O<sub>3</sub> and sodium ionophore X as sensing materials, respectively (Fig. 4b). The working mechanism of the device involves modulating the MOS-FET's electrical characteristics based on the concentration

of target ions in the solution. This integration of sensing and neuronal functions in a single device enables the artificial gustatory neuron to act as an input neuron in a spiking neural network (SNN), forming a neuromorphic-based E-tongue system. The neuromorphic architecture allows for spike-based data transmission and eliminates the need for heavy hardware components, resulting in reduced hardware requirements, lower energy consumption, and a highly scalable and energy-efficient system. With significantly lower power consumption compared to conventional taste sensors, the artificial gustatory neuron is well suited for practical implementation in IoT and mobile devices, opening up new possibilities for more advanced and efficient taste-sensing systems [64].

Inspired by the biological taste-sensing mechanism, recent studies have focused on integrating actual taste receptor proteins or taste-sensing cells with electronic devices to develop high-performance bioelectronic tongues. Notably, the use of human taste receptor domains has emerged as a promising approach to closely mimic human taste perception. By incorporating these receptor domains, bioelectronic tongues can achieve remarkable sensitivity. Figure 4c demonstrates an example of such an approach, where Jeong et al. developed an ultrasensitive bioelectronic tongue for the specific detection of sweet substances by utilizing the venus flytrap (VFT) domain of the human sweet taste receptor T1R2. This work differs from previous artificial electronic tongues using a specific, functionally relevant component of the human sweet taste receptor instead of other organic materials or whole receptor molecules. The authors addressed the limitations of expressing the whole sweet taste receptor due to its large and complex heterodimeric structure by overexpressing only the T1R2 VFT domain in a bacterial system. The T1R2 VFT was then immobilized on the floating electrodes of a carbon nanotube field-effect transistor (CNT-FET) to build the bioelectronic tongue device. This innovative approach allowed for the development of a highly sensitive and selective device for the detection of sweet substances, with the ability to detect them in complex environments such as commercial beverages. Furthermore, the device could measure the functional modulation of the human sweet receptor by enhancers and inhibitors, demonstrating its potential for various applications in the food industry and basic research [63].

Conventional bioelectronic tongues have limitations in detecting astringency, as they rely on specific target-binding methods that are not suitable for perceiving astringency, which is an indirect stimulation of mechanoreceptors in the tongue. In addition, they face challenges in achieving bitter-specific detection due to limitations such as the taste gap between species or the need for complex cell transfection and sensor surface modifications when using rodent taste cells or human taste receptors expressed in heterologous

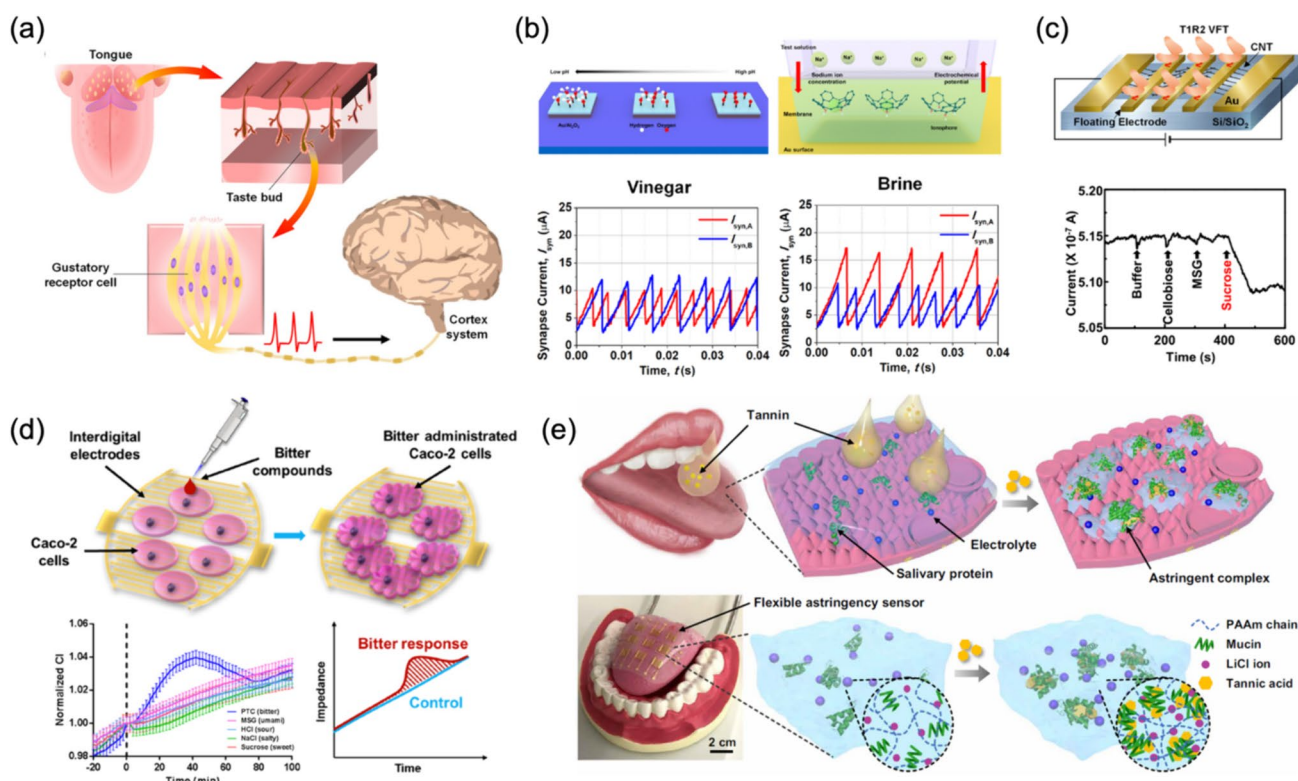


**Fig. 4** Taste sensors mimicking human gustatory system. **a** Chemical-induced action potential generation in human gustatory neurons for signal transmission to the brain. **b** Comparison of synaptic current and spiking frequency from artificial gustatory neurons between vinegar and brine. Reproduced from Ref. [64]. Copyright 2022, American Chemical Society. **c** Bioelectronic tongue using T1R2 Venus flytrap domain for selective sweet substance detection and differentiation from nonsweet tastants. Reproduced from Ref. [63]. Copyright

2022, American Chemical Society. **d** Bitter compound-induced morphological changes and increased cell-electrode impedance detection by the bioelectronic tongue. Reproduced from Ref. [58]. Copyright 2019, Elsevier. **e** Astringency sensing by a soft and flexible hydrogel-based artificial tongue mimicking the human sensing mechanism. Reproduced from Ref. [65]. Copyright 2020, American Association for the Advancement of Science

systems like HEK-293 cells. To address these challenges and expand the capabilities of bioelectronic tongues, Qin et al. developed a novel bioelectronic tongue (BioET) that specifically targets the detection of N–C=S-containing compounds, which are agonists of the human bitter taste receptor T2R38 (Fig. 4d). The authors utilized human Caco-2 cells, which endogenously express the T2R38 receptor, as the primary sensing element, and an interdigitated impedance sensor as the secondary transducer. The activation of T2R38 by bitter compounds induces morphological changes in the cells, which can be detected by electric cell-substrate impedance sensing (ECIS) with high sensitivity and selectivity. This BioET demonstrates the potential for identifying and screening receptor-specific bitter compounds, making it highly valuable for applications in the pharmaceutical and food industries [58].

Previous artificial tongues for astringency detection have shown poor performance, such as low selectivity and narrow detection range, due to the unique sensing mechanism of astringency, which involves the indirect stimulation of

mechanoreceptors through the complexation of ingested astringent foods and the salivary film. Moreover, a fully flexible and soft artificial tongue that is highly selective to specific astringent tastants has not yet been demonstrated. Yeom et al. developed a soft and flexible hydrogel-based artificial tongue inspired by the human sensing mechanism of astringency (Fig. 4e). The artificial tongue mimics the thin salivary layer on the human tongue using a soft and thin hydrogel film integrated on a flexible polymer substrate. The hydrogel consists of mucin as a secreted protein, lithium chloride as an electrolyte, and polyacrylamide as a 3D porous polymer network. When exposed to astringent compounds such as tannic acid (TA), the TA molecules bind with mucin to form hydrophobic aggregates, transforming the microporous hydrogel into a hierarchical micro/nanoporous structure. This unique transformation enhances ionic conductivity, enabling the detection of TA over a wide range (0.0005 to 1 wt%) with high sensitivity ( $0.292 \text{ wt\%}^{-1}$ ) and a fast response time ( $\sim 10 \text{ s}$ ). The remarkable achievements of the hydrogel-based artificial tongue in detecting astringency

open up new possibilities for the development of flexible and soft bioelectronic tongues specifically designed for sensing astringent compounds. This innovative approach has the potential to be integrated into a wide range of fields, such as food industry, healthcare monitoring, and robotics [65] (Table 3)

### Applications of Artificial Sensors in User-Interactive Interfaces

Human-inspired tactile sensors are crucial for advancing human–machine interfaces, aiming to mimic the sophisticated touch perception of human skin, enabling machines to interact more naturally and safely with their environment and with humans. The ability to detect and respond to various tactile stimuli, especially object softness, is essential for tasks ranging from delicate object manipulation. Qiu et al. developed a multisensory electronic skin that combines piezoelectric and piezoresistive sensors, emulating the FA and SA mechanoreceptors found in human skin (Fig. 5a). This dual-mode sensing allows for both dynamic and static stimuli detection, crucial for natural object interaction. The system employs a two-step, non-destructive softness measurement process inspired by human touch: first, a light contact for initial classification using piezoelectric sensing, followed by appropriate force application for quantitative measurement via strain sensing. This biomimetic approach, enhanced by machine learning algorithms for data processing, enables the system to adaptively control grasping force based on object softness, much like human hands. By closely replicating human tactile perception, the system achieves more intuitive and versatile object manipulation, a key

requirement for advanced human–machine interfaces in applications ranging from prosthetics to robotic surgery [66].

Building upon this advancement in tactile sensing, dynamic HMI devices, as a key role of use-interactive interfaces between human and machine, further enable to deliver the user intention to the machine interface through the physical information such as low-frequency touch or hand motions and voices, corresponding to 1 to 10 and 10 to 2000 Hz, respectively [67, 68]. Therefore, HMI devices are required to perceive a wide range of frequency bands, as well as possessing the capability to exhibit selective response characteristics to specific frequencies with a high signal-to-noise ratio. Human cochlear-inspired frequency-selective acoustic sensors allow sound-driven robot control, which is meaningful in human–machine interfaces. Recent advancements in this field include the development of highly sensitive and selective acoustic sensors that can discriminate between different sound frequencies, enabling precise control of robotic systems. Park et al. developed a frequency-selective triboelectric sensor (TES) based on a hierarchical ferroelectric composite with macrodome, micropore, and nanoparticle structures (Fig. 5b). The authors demonstrated the application of their frequency-selective TESs in a sound-driven human–machine interface (HMI) system for remote control and continuous real-time manipulation. They used four different acoustic frequency ranges to operate robotic hands with different finger grasping motions. The versatile robotic hand motions could be wirelessly controlled using specific input sound frequencies, and due to the high acoustic frequency selectivity, the sound-driven HMI could only be operated by the designated frequency, allowing accurate manipulation without interference from complex frequency inputs. This application showcases the potential of

**Table 3** Summary of taste sensors mimicking human gustatory system

Taste	Mechanism	Materials and structure	Sensing performances	References
Bitterness	Activation of T2R38 by bitter compounds	Caco-2 cell (express the T2R38 receptor)	1 $\mu\text{M}$ –1 mM (both * PTC and ** PROP) Limit of detection: 0.09352 $\mu\text{M}$ for PTC/0.8404 $\mu\text{M}$ for PROP	[58]
Sweetness	Conformational changes in venus fly-trap (VFT) domain of human T1R2 sweet receptor	T1R2 VFT immobilized on the floating electrode with carbon nanotube field-effect transistor (CNT-FET)	0.1 fM–1 $\mu\text{M}$	[63]
Sourness/saltiness	Surface charge difference based on ion concentration	$\text{Al}_2\text{O}_3/\text{Au}$ (sourness) Sodium ionophore X in PVC membrane/Au (Saltiness)	150 Hz/pH (pH 3–9) 120 Hz/dec ( $10^{-4}$ – $10^{-1}$ M)	[64]
Astringency	Ionic conductivity changes from transformation of porous structure induced by binding between tannic acid and mucin	Polyacrylamide (PAAm) hydrogel/mucin proteins/LiCl electrolyte	0.0005–1 wt% tannic acid 0.292/wt%	[65]

\*PTC: phenylthiocarbamide

\*\*PROP: propylthiouracil

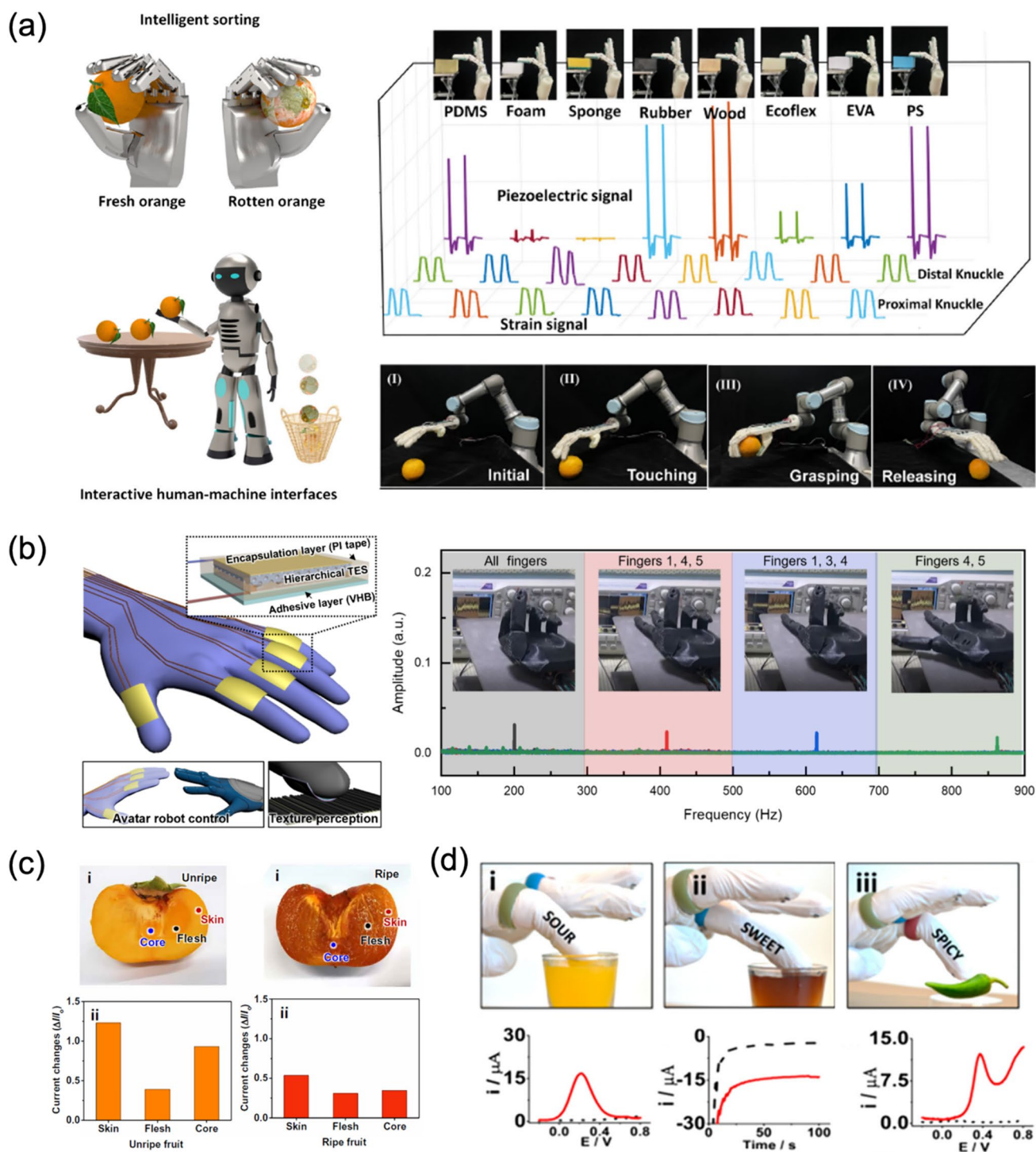


**Fig. 5** Applications of artificial sensors in user-interactive interfaces. **a** Intuitive object manipulation using multisensory pressure sensor mimicking FA/SA mechanoreceptor for interactive HMI. Reproduced from Ref. [66]. Copyright 2022, Springer Nature. **b** Frequency-selective robotic hand motion control for dynamic HMI. Reproduced from Ref. [50]. Copyright 2022, American Association for the

Advancement of Science. **c** Standardization of astringency for evaluating fruit ripeness. Reproduced from Ref. [65]. Copyright 2020, American Association for the Advancement of Science. **d** Automated taste discrimination in various food samples. Reproduced from Ref. [14]. Copyright 2018, American Chemical Society

frequency-selective acoustic sensors in developing advanced human–machine interfaces for remote control and real-time manipulation in noisy environments.

The sense of taste, along with touch and hearing, plays an essential role in delivering intuitive sensory information in user-interactive interfaces and assessing the quality and safety of food and beverages in our daily lives. Recent advancements in biomimetic taste sensors have led to the development of artificial tongues that can mimic the human sense of taste [56–65]. For example, the flexible hydrogel-based artificial tongue shows promise in taste-sensing applications, such as standardized astringency evaluation in beverages and monitoring fruit ripeness (Fig. 5c). Its wipe-and-detect functionality enables direct analysis on curved surfaces, expanding its potential for on-site quality control. The development of a portable 3×3 sensor array for taste mapping highlights the potential for creating compact, user-friendly electronic tongues for various industries [65]. Furthermore, the integration of an artificial electronic tongue with a robotic hand enables automated taste discrimination in various food samples. The robotic fingers, equipped with printed electrochemical sensors, can detect and differentiate between sweetness, sourness, and spiciness in liquid food samples by analyzing the distinct electrochemical signatures generated upon immersion. In addition, the system can discriminate tastes in solid food items by employing a conductive agarose gel on the robotic fingers, facilitating sample collection and electrochemical analysis (Fig. 5d). The artificial tongue-integrated robotic hand can also distinguish between caffeinated/decaffeinated beverages and sugar/sugar-free drinks, as well as quantify glucose content in beverages. This integration allows for rapid, on-site flavor screening of a wide array of food items through a simple “touching” and “sensing” approach, making it suitable for applications in food quality control, human–robot interaction, and assisted food preparation and consumption [14].

## Conclusion

This review highlights recent advancements in artificial sensory electronics inspired by human somatosensory systems, particularly focusing on tactile, hearing, and taste sensing, and their applications in user-interactive interfaces. In tactile sensing, distinguishing static and dynamic pressure is essential for intuitive user-interactive interfaces and accurate manipulation. Traditional pressure sensors faced limitations in detecting combined tactile information. To overcome these challenges, pressure sensors mimicking FA/SA mechanoreceptors have been developed, combining hybrid signal transduction mechanisms and material optimization. These advancements enable effective static and dynamic pressure sensing, enhancing interaction between wearers

and devices. Artificial acoustic sensors, essential for remote machine control and voice recognition, face challenges in detecting desired frequencies among background noise. Recent research has produced frequency-selective sensors inspired by the human cochlea, achieving high selectivity and sensitivity. Miniaturized sensors mimicking cochlear structures, from basilar membranes to hair cells, have been developed, offering broad frequency selectivity and high sensitivity across the human audible range. These advancements improve noise reduction, signal processing, and overall sensitivity, with applications in hearing aids, dynamic human–machine interfaces, and biometric authentication. In gustatory sensing, artificial taste sensors emulate human taste perception by drawing inspiration from taste buds and receptors. Recent developments include integrating taste receptor proteins or cells into electronic devices and using materials mimicking human taste receptor responses. These developments enhance selectivity, detectable concentration range, sensitivity, and response time, addressing issues such as high-energy consumption and low selectivity.

While challenges remain, such as further miniaturization and performance enhancement in complex environments, these bio-inspired artificial electronics have significantly improved user-interactive interfaces in applications such as robotic object manipulation, sound-driven human–machine interactions, and automated taste discrimination in food analysis. Future research will likely focus on multimodal sensory integration systems, creating more comprehensive and realistic sensory experiences in conjunction with haptic interface. The convergence of these bio-inspired sensors with other cutting-edge technologies promises to revolutionize human–machine interfaces, leading to more intuitive and immersive user experiences across various fields such as tele-haptics and VR/AR interfaces.

**Acknowledgements** This work was supported by the National Research Foundation (NRF) of Korea (2021R1A2C3009222, 2022M3H4A1A02076825), and the Ministry of Trade, Industry and Energy (20010566).

## References

1. Y. Luo, M. Abidian, J. Ahn, D. Akinwande, A. Andrews, M. Antonietti, Z. Bao, M. Berggren, C. Berkey, C. Bettinger, J. Chen, P. Chen, W. Cheng, X. Cheng, S. Choi, A. Chortos, C. Dagdeviren, R. Dauskardt, C. Di, M. Dickey, X. Duan, A. Facchetti, Z. Fan, Y. Fang, J. Feng, X. Feng, H. Gao, W. Gao, X. Gong, C. Guo, X. Guo, M. Hartel, Z. He, J. Ho, Y. Hu, Q. Huang, Y. Huang, F. Huo, M. Hussain, A. Javey, U. Jeong, C. Jiang, X. Jiang, J. Kang, D. Karnaushenko, A. Khademhosseini, D. Kim, I. Kim, D. Kireev, L. Kong, C. Lee, N. Lee, P. Lee, T. Lee, F. Li, J. Li, C. Liang, C. Lim, Y. Lin, D. Lipomi, J. Liu, K. Liu, N. Liu, R. Liu, Y. Liu, Y. Liu, Z. Liu, Z. Liu, X. Loh, N. Lu, Z. Lv, S. Magdassi, G. Malliaras, N. Matsuhisa, A. Nathan, S. Niu, J. Pan, C. Pang, Q. Pei, H. Peng, D. Qi, H. Ren, J. Rogers, A. Rowe,

- O. Schmidt, T. Sekitani, D. Seo, G. Shen, X. Sheng, Q. Shi, T. Someya, Y. Song, E. Stavrinidou, M. Su, X. Sun, K. Takei, X. Tao, B. Tee, A. Thean, T. Trung, C. Wan, H. Wang, J. Wang, M. Wang, S. Wang, T. Wang, Z. Wang, P. Weiss, H. Wen, S. Xu, T. Xu, H. Yan, X. Yan, H. Yang, L. Yang, S. Yang, L. Yin, C. Yu, G. Yu, J. Yu, S. Yu, X. Yu, E. Zamburg, H. Zhang, X. Zhang, X. Zhang, X. Zhang, Y. Zhang, Y. Zhang, S. Zhao, X. Zhao, Y. Zheng, Y. Zheng, Z. Zheng, T. Zhou, B. Zhu, M. Zhu, R. Zhu, Y. Zhu, Y. Zhu, G. Zou, X. Chen, *ACS Nano* **17**, 5211–5295 (2023)
2. J. Park, Y. Lee, S. Cho, A. Choe, J. Yeom, Y.G. Ro, J. Kim, D. Kang, S. Lee, H. Ko, *Chem. Rev.* **124**, 1464–1534 (2024)
  3. H. Xia, Y. Zhang, N. Rajabi, F. Taleb, Q. Yang, D. Kragic, Z. Li, *Nat. Commun.* **15**, 1760 (2024)
  4. T.-H. Yang, J.R. Kim, H. Jin, H. Gil, J.-H. Koo, H.J. Kim, *Adv. Funct. Mater.* **31**, 2008831 (2021)
  5. M. Zhu, Z. Sun, Z. Zhang, Q. Shi, T. He, H. Liu, T. Chen, C. Lee, *Sci. Adv.* **6**, eaaz8693 (2020)
  6. Y. Liu, C. Yiu, Z. Song, Y. Huang, K. Yao, T. Wong, J. Zhou, L. Zhao, X. Huang, S. Nejad, M. Wu, D. Li, J. He, X. Guo, J. Yu, X. Feng, Z. Xie, X. Yu, *Sci. Adv.* **8**, eab16700 (2022)
  7. Y.H. Jung, B. Park, J.U. Kim, T. Kim, *Adv. Mater.* **31**, 1803637 (2019)
  8. Y. Lee, J. Park, A. Choe, S. Cho, J. Kim, H. Ko, *Adv. Funct. Mater.* **30**, 1904523 (2020)
  9. A. Bag, G. Ghosh, M. Sultan, H. Choudhry, S. Hong, T. Trung, G. Kang, N. Lee, *Adv. Mater.* (2024)
  10. R.N. Albustanji, S. Elmanaseer, A. Alkhatib, *Robotics* **12**, 68 (2023)
  11. H. Jin, Y. Kim, W. Youm, Y. Min, S. Seo, C. Lim, C. Hong, S. Kwon, G. Park, S. Park, H. Kim, *npj Flex. Electron.* **6**, 82 (2022)
  12. H. Guo, X. Pu, J. Chen, Y. Meng, M. Yeh, G. Liu, Q. Tang, B. Chen, D. Liu, S. Qi, C. Wu, C. Hu, J. Wang, Z. Wang, *Sci. Robot.* **3**, 2516 (2018)
  13. Q. Zhang, Y. Wang, D. Li, J. Xie, R. Tao, J. Luo, X. Dai, H. Torun, Q. Wu, W. Ng, R. Binns, Y. Fu, *Microsyst. Nanoeng.* **8**, 99 (2022)
  14. B. Ciui, A. Martin, R. Mishra, T. Nakagawa, T. Dawkins, M. Lyu, C. Cristea, R. Sandulescu, J. Wang, *ACS Sens.* **3**(11), 2375–2384 (2018)
  15. M. Zniber, P. Vahdatiyekta, T.P. Huynh, *Biosens. Bioelectron.* **219**, 114810 (2023)
  16. L. Yang, Z. Wang, S. Zhang, Y. Li, C. Jiang, L. Sun, W. Xu, *Nano Lett.* **23**(1), 8–16 (2023)
  17. M.A. Yahya, A. Dahanayake, *Appl. Sci.* **11**(17), 7978 (2021)
  18. T. Narumi, S. Nishizaka, T. Kajinami, T. Tanikawa and M. Hirose, In: Proceedings of the SIGCHI Conference on Human Factors in Computing Systems, Vancouver, BC, Canada, 7–12 May 2011; Association for Computing Machinery: New York, NY, USA, pp. 93–102. (2011)
  19. A. Nijholt, C. Velasco, G. Huisman and K. Karunanayaka, MHFI '16: Proceedings of the 1st Workshop on Multi-sensorial Approaches to Human-Food Interaction 1–6 (2016)
  20. H. Kim, Y.T. Kwon, H.R. Lim, J.H. Kim, Y.S. Kim, W.H. Yeo, *Adv. Funct. Mater.* **31**, 2005692 (2021)
  21. T. Sun, B. Feng, J. Huo, Y. Xiao, W. Wang, J. Peng, Z. Li, C. Du, W. Wang, G. Zou, L. Liu, *Nano-Micro Lett.* **16**, 14 (2024)
  22. L. Gu, S. Poddar, Y. Lin, Z. Long, D. Zhang, Q. Zhang, L. Shu, X. Qiu, M. Kam, A. Javey, Z. Fan, *Nature* **581**, 278–282 (2020)
  23. Y. Liu, C. Yiu, Z. Zhao, W. Park, R. Shi, X. Huang, Y. Zeng, K. Wang, T. Wong, S. Jia, J. Zhou, Z. Gao, L. Zhao, K. Yao, J. Li, C. Sha, Y. Gao, G. Zhao, Y. Huang, D. Li, Q. Guo, Y. Li, X. Yu, *Nat. Commun.* **14**, 2297 (2023)
  24. M. Liu, Y. Zhang, J. Wang, N. Qin, H. Yang, K. Sun, J. Hao, L. Shu, J. Liu, Q. Chen, P. Zhang, and T. Tao *Nat. Commun.* **13**, 79 (2022)
  25. Y. Li, X. Wei, Y. Zhou, J. Wang, R. You, *Microsyst. Nanoeng.* **9**, 129 (2023)
  26. C. Choi, M.K. Choi, S. Liu, M. Kim, O.K. Park, C. Im, J. Kim, X. Qin, G.J. Lee, K.W. Cho, M. Kim, E. Joh, J. Lee, D. Son, S.-H. Kwon, N.L. Jeon, Y.M. Song, N. Lu, D.-H. Kim, *Nat. Commun.* **8**, 1664 (2017)
  27. Z. Long, Y. Ding, S. Poddar, Q. Zhang, Z. Fan, *Mater. Today Electron* **6**, 100071 (2023)
  28. B. Malnic, J. Hirono, T. Sato, L.B. Buck, *Cell* **96**(5), 713–723 (1999)
  29. C. Qin, Y. Wang, J. Hu, T. Wang, D. Liu, J. Dong, Y. Lu, *Adv. Sci.* **10**, 2204726 (2023)
  30. R.S. Johansson, J.R. Flanagan, *Nat. Rev. Neurosci.* **10**, 345–359 (2009)
  31. M. Park, B.G. Bok, J.H. Ahn, M.S. Kim, *Micromachines* **9**, 321 (2018)
  32. J. Park, Y. Lee, J. Hong, M. Ha, Y. Jung, H. Lim, S. Kim, H. Ko, *ACS Nano* **8**, 4689 (2014)
  33. J. Park, Y. Lee, J. Hong, M. Ha, Y. Jung, H. Lim, S. Kim, H. Ko, *ACS Nano* **8**, 12020 (2014)
  34. J. Park, Y. Lee, S. Lim, Y. Lee, Y. Jung, H. Lim, H. Ko, *BioNano Science* **4**, 349 (2014)
  35. M. Ha, S. Lim, J. Park, D.S. Um, Y. Lee, H. Ko, *Adv. Funct. Mater.* **25**, 2841–2849 (2015)
  36. C. Choong, M. Shim, B. Lee, S. Jeon, D. Ko, T. Kang, J. Bae, S. Lee, K. Byun, J. Im, Y. Jeong, C. Park, J. Park, U. Chung, *Adv. Mater.* **26**, 3451–3458 (2014)
  37. J. Park, M. Kim, Y. Lee, H.S. Lee, H. Ko, *Sci. Adv.* **1**, e1500661 (2015)
  38. H.Q. Huynh, T.Q. Trung, A. Bag, T.D. Do, M.J. Sultan, M. Kim, N.E. Lee, *Adv. Funct. Mater.* **33**, 2303535 (2023)
  39. S. Chun, J. Kim, Y. Yoo, Y. Choi, S. Jung, D. Jang, G. Lee, K. Song, K. Nam, I. Youn, D. Son, C. Pang, Y. Jeong, H. Jung, Y. Kim, B. Choi, J. Kim, S. Kim, W. Park, S. Park, *Nat. Electron.* **4**, 429–438 (2021)
  40. K.Y. Chun, Y.J. Son, E.S. Jeon, S. Lee, C.S. Han, *Adv. Mater.* **30**, 1706299 (2018)
  41. D. Lipomi, M. Vosgueritchian, B. Tee, S. Hellstrom, J. Lee, C. Fox, Z. Bao, *Nat. Nanotechnol.* **6**, 788 (2011)
  42. J. Ge, L. Sun, F.R. Zhang, Y. Zhang, L.A. Shi, H.Y. Zhao, H.W. Zhu, H.L. Jiang, S.H. Yu, *Adv. Mater.* **28**, 722 (2016)
  43. X. Wu, J. Zhu, J.W. Evans, A.C. Arias, *Adv. Mater.* **32**, 2005970 (2020)
  44. Y. Dobashi, D. Yao, Y. Petel, T. Nguyen, M. Sarwar, Y. Thabet, C. Ng, E. Glitz, G. Nguyen, C. Plesse, F. Vidal, C. Michal, J. Madden, *Science* **376**, 502–507 (2022)
  45. S. Lee, W. Kim, N.C. Park, J.W. Park, *Adv. Funct. Mater.* **33**, 2306026 (2023)
  46. J.H. Han, J.H. Kwak, D.J. Joe, S.K. Hong, H.S. Wang, J.H. Park, S. Hur, K.J. Lee, *Nano Energy* **53**, 198–205 (2018)
  47. H. Ahmadi, H. Moradi, C.J. Pastras, S. Abolpour Moshizi, S. Wu, M. Asadnia, *ACS Appl. Mater. Interfaces* **13**(37), 44904–44915 (2021)
  48. Z. Xiang, L. Li, Z. Lu, X. Yu, Y. Cao, M. Tahir, Z. Yao, Y. Song, *Matter* **6**, 554–569 (2023)
  49. J. Jang, J.H. Jang, H. Choi, *Adv. Healthc. Mater.* **6**, 1700674 (2017)
  50. J. Park, D.-H. Kang, H. Chae, S.K. Ghosh, C. Jeong, Y.J. Park, S. Cho, Y. Lee, J. Kim, Y. Ko, J.J. Kim, H. Ko, *Sci. Adv.* **8**, abj9220 (2022)
  51. H.S. Lee, J. Chung, G.-T. Hwang, C.K. Jeong, Y. Jung, J.-H. Kwak, H. Kang, M. Byun, W.D. Kim, S. Hur, S.-H. Oh, K.J. Lee, *Adv. Funct. Mater.* **24**, 6914–6921 (2014)
  52. H.S. Wang, S.K. Hong, J.H. Han, Y.H. Jung, H.K. Jeong, T.H. Im, C.K. Jeong, B.-Y. Lee, G. Kim, C.D. Yoo, K.J. Lee, *Sci. Adv.* **7**, abe5683 (2021)
  53. J. Chandrashekar, M.A. Hoon, N.J.P. Ryba, C.S. Zuker, *Nature* **444**(7117), 288–294 (2006)

54. Y. Zhang, M.A. Hoon, J. Chandrashekar, K.L. Mueller, B. Cook, D. Wu, C.S. Zuker, N.J.P. Ryba, *Cell* **112**(3), 293–301 (2003)
55. G.Q. Zhao, Y. Zhang, M.A. Hoon, J. Chandrashekar, I. Erlenbach, N.J.P. Ryba, C.S. Zuker, *Cell* **115**(3), 255–266 (2003)
56. S. Ghosh, A. Pannone, D. Sen, A. Wali, H. Ravichandran, S. Das, *Nat. Commun.* **14**, 6021 (2023)
57. C. Qin, Z. Qin, D. Zhao, Y. Pan, L. Zhuang, H. Wan, A.D. Pizio, E. Malach, M.Y. Niv, L. Huang, N. Hu, P. Wang, *Talanta* **199**, 131–139 (2019)
58. Z. Miao, H. Tan, L. Gustavsson, Y. Zhou, Q. Xu, O. Ikkala, B. Peng, *Smell* **20**(7), 2305195 (2024)
59. J. Liu, J. Qian, M. Adil, Y. Bi, H. Wu, X. Hu, Z. Wang, W. Zhang, *Microsyst. Nanoeng.* **10**, 57 (2024)
60. X. Wei, B. Wang, X. Cao, H. Zhou, Z. Wu, Z.L. Wang, *Nat. Food* **4**, 721–732 (2023)
61. X. Wu, K. Toko *Trends. Analyt. Chem.* **158**, 116874 (2023)
62. M.D. Wagh, S.K. Sahoo, S. Goel, *Sens. Actuator A Phys.* **333**, 113301 (2022)
63. J.Y. Jeong, Y.K. Cha, S.R. Ahn, J. Shin, Y. Choi, T.H. Park, S. Hong, A.C.S. *Appl. Mater. Interfaces* **14**(2), 2478–2487 (2022)
64. J.K. Han, D.M. Geum, M.W. Lee, J.M. Yu, S.K. Kim, S. Kim, Y.K. Choi, *Nano Lett.* **22**(13), 5244–5251 (2022)
65. J. Yeom, A. Choe, S. Lim, Y. Lee, S. Na, H. Ko, *Sci. Adv.* **6**, eaba5785 (2020)
66. Y. Qin, S. Sun, X. Wang, K. Shi, Z. Wang, X. Ma, W. Zhang, G. Bao, Y. Tian, Z. Zhang, H. Ding, H. Chai, A. Liu, H. Wu, *npj Flex. Electron.* **6**, 45 (2022)
67. S. Jung, J.H. Kim, J. Kim, S. Choi, J. Lee, I. Park, T. Hyeon, D.H. Kim, *Adv. Mater.* **26**, 4825–4830 (2014)
68. Y. Liu, J.J.S. Norton, R. Qazi, Z. Zou, K.R. Ammann, H. Liu, L. Yan, P.L. Tran, K.-I. Jang, J.W. Lee, D. Zhang, K.A. Kilian, S.H. Jung, T. Bretl, J. Xiao, M.J. Slepian, Y. Huang, J.-W. Jeong, J.A. Rodgers, *Sci. Adv.* **2**, e1601185 (2016)

**Publisher's Note** Springer Nature remains neutral with regard to jurisdictional claims in published maps and institutional affiliations.

Springer Nature or its licensor (e.g. a society or other partner) holds exclusive rights to this article under a publishing agreement with the author(s) or other rightsholder(s); author self-archiving of the accepted manuscript version of this article is solely governed by the terms of such publishing agreement and applicable law.